JOURNAL OF SOLID STATE CHEMISTRY 95, 388–396 (1991)

The Structural Consequences of the Chemical Reaction of $YBa_2Cu_3O_{7-y}$ with *n*-Butyl Lithium

M. A. SEÑARÍS-RODRÍGUEZ, C. J. D. HETHERINGTON, A. VÁREZ, E. MORÁN, AND M. A. ALARIO-FRANCO*

Departamento de Química Inorgánica, Facultad de Ciencias Químicas, Universidad Complutense, 28040-Madrid, Spain

Received December 10, 1990; in revised form May 13, 1991; in final form September 20, 1991

HREM has been used to study the processes induced by the reaction of the HTSC $YBa_2Cu_3O_{7-y}$ (commonly referred to as "123") with the lithiating agent *n*-BuLi. High resolution electron micrographs reveal that this reaction promotes, *at room temperature*, irreversible microstructural modifications into the "123" structure leading to a rather heterogeneous product. In this respect, both the "247" ($Y_2Ba_4Cu_7O_{15-z}$) and the "124" ($YBa_2Cu_4O_8$) structures appear as either extended defects within the "123" matrix or disordered intergrowths. A structural model is proposed to justify the high lithium conductivity displayed by these materials. © 1991 Academic Press, Inc.

Introduction

Following our previous work, both on lithium insertion in reduced tungsten oxides (*1*, *2*) and on superconducting materials such as $ReBa_2Cu_3O_{7-y}$ (*Re*: rare earth) (*3–5*), we have prepared materials consisting of $YBa_2Cu_3O_{7-y}$ reacted with *n*-BuLi. In these materials, for lithium to "123" nominal molar ratios Li/"123" ≤ 1.2, superconductivity is maintained and T_c is kept rather high ($T_c \simeq 90$ K), while lithium ionic conductivity appears at $T \geq 400$ K (*6*, *7*).

By means of X-ray diffraction, we have observed that the reaction of the lithiating agent with the original $YBa_2Cu_3O_{7-y}$ induces irreversible structural modifications in the "123" phase (*7*). As it was difficult to characterize those transformations just from powder X-ray diffraction data, we have undertaken an electron diffraction and HREM study in the obtained materials. These results are presented here.

We may mention here that an electrochemical study of the lithium insertion into "123" has recently appeared (*8*); however, it does not include any structural discussion.

Experimental

The materials were obtained by reacting $YBa_2Cu_3O_{7-y}$ samples with solutions of *n*-BuLi in hexane in the appropriate conditions (*7*). The approximate formal Li/"123" molar ratio was established by readily extracting lithium from the samples using an iodine solution in acetonitrile and taking into account the amount of $YBa_2Cu_3O_{7-y}$ sample

* To whom correspondence should be addressed.

0022-4596/91 $3.00

Copyright © 1991 by Academic Press, Inc.
All rights of reproduction in any form reserved.

used. As the reacted samples are not fully homogeneous (see below) it is best not to elaborate on their formulas.

Specimens for transmission electron microscopy were prepared by grinding, dispersing in dry *n*-hexane, and putting a few droplets on either a carbon-coated nylon or copper grid; they were only exposed to the atmosphere while the grid was mounted in the sample holder. High resolution electron microscopy and electron diffraction were performed on a JEOL 4000 EX instrument operated at 400 kV. All the high resolution images were obtained under conditions close to the Scherzer defocus, in which the projection of atomic columns appears black on a white background. The amounts of Ba, Y, and Cu in the constituent phases in the various samples were determined by X-ray microanalysis using a JEOL 2000 FX TEMSCAN analytical electron microscope operating at 200 kV.

The presence of lithium in the crystals was detected by electron energy loss spectroscopy (EELS), using a ZEISS 902 electron microscope working at 80 kV and fitted with a prism–mirror–prism type electron spectrometer.

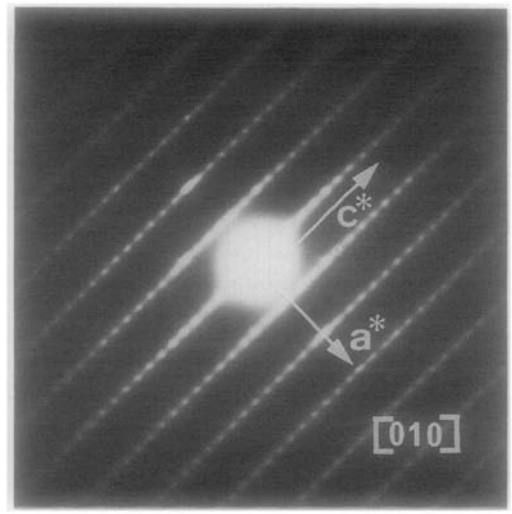

FIG. 1. Electron diffraction pattern of a sample with relatively low lithium to "123" molar ratio, Li/"123" $\simeq$ 0.38, along the [010] zone axis. Marked streaking along the c^*-axis is apparent.

Results

I. Samples with low lithium to "123" molar ratio (Li/"123" $\leq$ 0.5). The electron diffraction patterns of the samples, in which the lithium to "123" molar ratio is low, show a marked streaking in all rows parallel to the c^*-axis (Fig. 1), while no extra spots or streaks are observed in other regions of the reciprocal cell. The corresponding electron micrographs, Fig. 2, show the presence of parallel, extended defects running perpendicular to the c-axis of the "123" matrix. These become more frequent as the Li/"123" relation increases. Detailed analysis of the high resolution images indicates that, in these defects, the basic Ba–Y–Ba perovskite blocks are similar to those of the "123" structure, but that they are separated by double $[CuO_4]$ chain layers along the c-axis; as the interplanar distance along that direction is d = 13.6 Å, it corresponds to half the cell of the "124" structure, Figs. 3B and 3C.

It is worth remembering here that there exists a close structural relationship between $YBa_2Cu_3O_{7-y}$ ("123"), $YBa_2Cu_4O_8$ ("124"), and $Y_2Ba_4Cu_7O_{15-z}$ ("247") (see Fig. 3); indeed, "247" can be considered as an ordered intergrowth of a unit cell of "123" phase and half a unit cell of "124". This means that an extended defect such as observed here, Fig. 2, consisting of half a unit cell of the "124" within the "123" matrix, can also be considered, in a first approximation, as half a unit cell of the "247." This kind of unit cell intergrowth is sometimes called a Wadsley defect (*9*). Obviously, if the number of these defects increases, they can constitute an ordered or disordered intergrowth within the parent

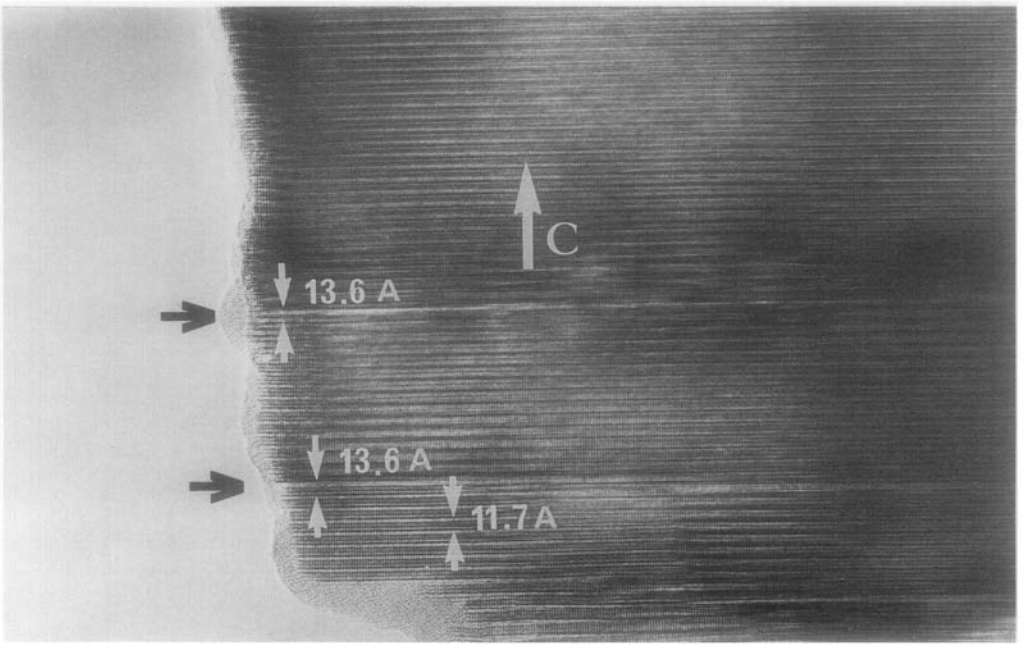

FIG. 2. High-resolution electron micrograph of the sample with a lithium to "123" molar ratio ≈ 0.38 along the [110] zone axis; black arrows show the presence of extended defects perpendicular to the c-axis of the "123" matrix, in which the interplanar distance $d_{[001]}$ is 13.6 Å.

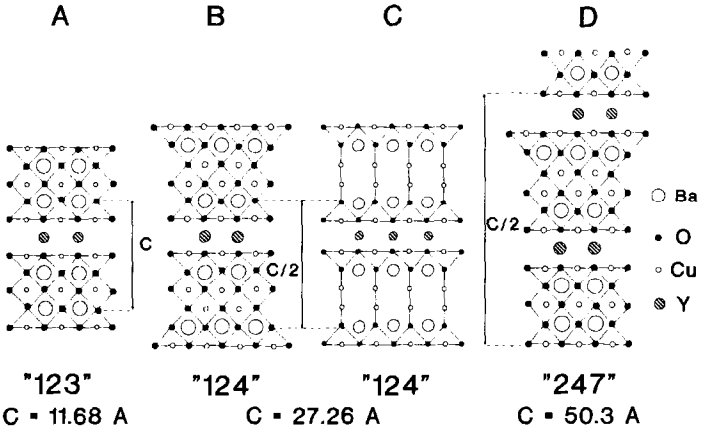

FIG. 3. Schematic illustration of the "123" (A), "124" (B, C), and "247" structures (D). In B we are looking at the "124" structure parallel to the [100] direction, so that the copper atoms in the double $[CuO_4]$ chain layers appear displaced by a translation of $\frac{1}{2}$ [011]; in C this same structure is viewed along the [010] zone axis, and in this orientation the copper atoms in the double $[CuO_4]$ chain layers appear related by a (001) pseudo-mirror plane.

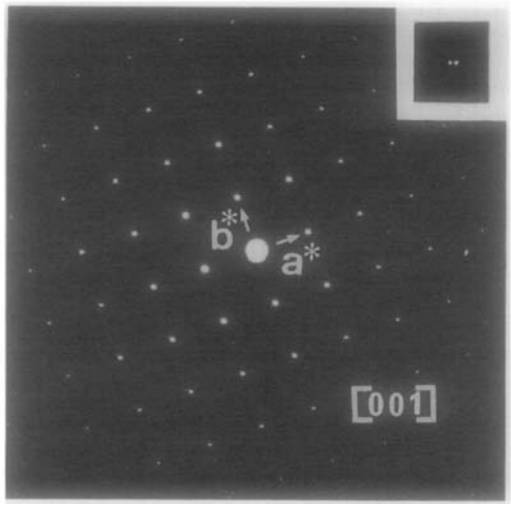

FIG. 4A. [001] diffraction pattern over a twinned area in the sample with a lithium to "123" molar ratio ≃ 1.2. The weak splitting of the outer spots is enlarged in the inset.

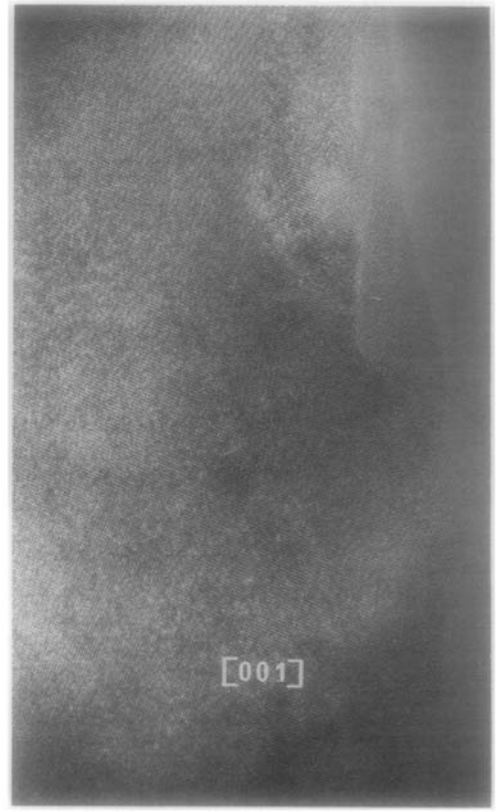

FIG. 4B. HREM image of the *a–b* plane of the sample with a lithium to "123" molar ratio ≃ 1.2.

structure. These considerations allowed us to identify the second phase appearing in the X-ray diffraction patterns of the sample with Li/"123" ≃ 0.38 as a $Y_2Ba_4Cu_7O_{15-z}$ ("247") type phase.

II. Samples with a higher lithium to "123" molar ratio (Li/"123" ≃ 1.2). The structure of the material with a high lithium to "123" molar ratio (Li/"123" ≃ 1.2) is markedly different. Its ED patterns and the corresponding images have to be interpreted on the basis of a twinned "124" structure (lattice parameters a = 3.842 Å, b = 3.871 Å, and c = 27.24 Å, Space Group *Ammm* (*10*), see below). Study of the *a–b* plane shows that this has not been affected by the reaction, and both electron diffraction patterns and micrographs along [001] do not show any disorder, Figs. 4A and 4B. It is worth noting that the A-centering of the "124" unit cell causes the reflections (*hk*0) to be absent for k = odd; nevertheless, in these samples, no extinctions are observed in the [001] diffraction pattern. This is due to both 90° rotation twins with rotation axis [001] and double diffraction. The slight (*hk*0) spot splitting which is visible at large g-values (see inset Fig. 4A) is indeed due to the twinning. ED patterns containing the c^*-axis, however, did show streaking parallel to it, Fig. 5A. The high-resolution electron micrographs showed that the structure is very strained and distorted and, even if an average periodicity to c remains, with d ≃ 27.2 Å, most fringes corresponding to the (001) planes are bent (Figs. 5B and 6). Moreover, high-resolution images containing the c-axis confirm that this material is twinned, with 90° rotation twins and rotation axis [001]. In this respect, in the region marked A in Fig. 7 the structure is imaged along the [100] direction and the copper atoms in the double $[CuO_4]$

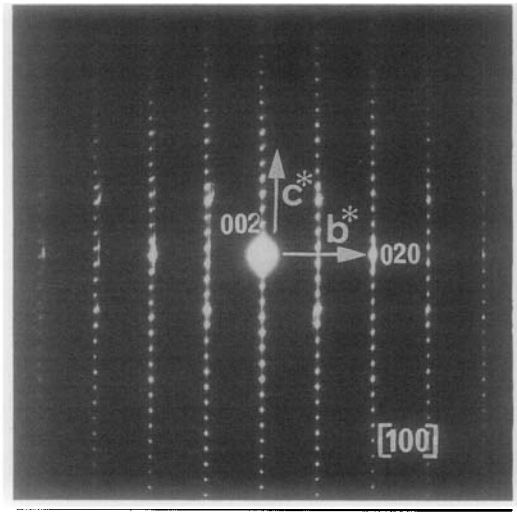

FIG. 5A. Electron diffraction pattern of the "124" structure present in the sample with a lithium to "123" molar ratio ≃ 1.2. The microcrystal is orientated along the [100] zone axis, so that the allowed reflections correspond to $0kl$ with $k + l = 2n$. Streaking is also apparent along the c^*-axis.

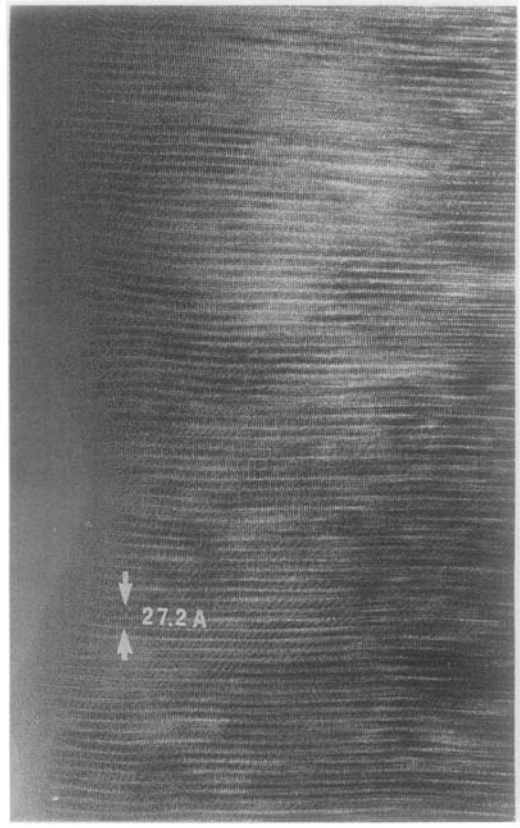

FIG. 5B. HREM image of the sample with a lithium to "123" molar ratio ≃ 1.2 in the [100] orientation. Notice the presence of the strained and distorted "124" structure.

chain layers appear displaced by a translation of 1/2 [011], while in the region marked B in the same figure the structure is imaged along the [010] direction and those copper atoms are related by a (001) pseudo-mirror plane (cf. Fig. 7 with Figs. 3B and 3C).

This sample, having a high lithium content, is also much more susceptible to beam damage and amorphization, and the crystal edge often appears structureless, Figs. 5B, 6, and 7.

On the basis of these results, the broad peaks appearing in the X-ray diffraction patterns corresponding to this material were approximately indexed with a "124"-type unit cell.

EELS analyses were performed on both the original "123" material and the same sample treated with *n*-BuLi. Qualitative comparison of the spectra show that they are equivalent except for the appearance of a new peak at ≃55 eV (corresponding to the lithium *K*-edge) in the spectra of the reacted material. This result confirms the presence of lithium together with yttrium, barium, copper, and oxygen in the lithiated sample (Fig. 8).

Discussion

This transmission electron microscopy study of $YBa_2Cu_3O_{7-y}$ samples reacted with *n*-BuLi indicates that this reaction induces the presence of extra CuO chain layers into the "123" structure. These extra chains appears as isolated defects for a low lithium to "123" molar ratio, Li/"123" ≤ 0.50, but give rise to microstructural intergrowths be-

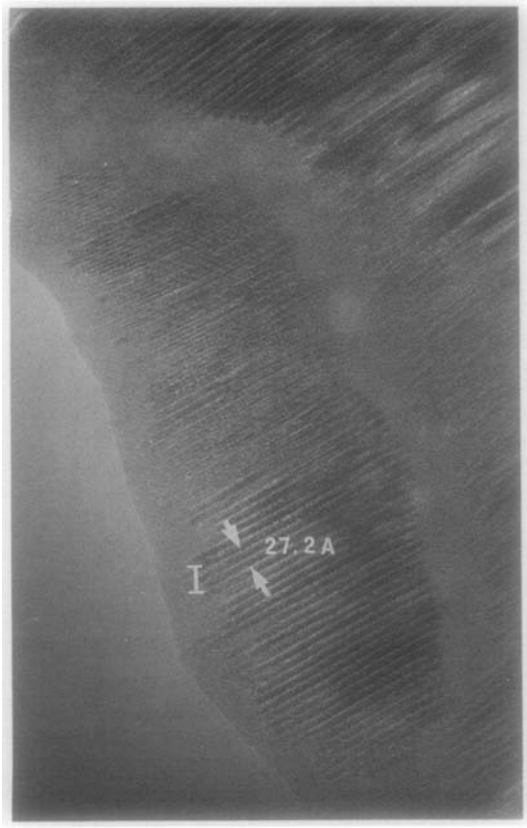

FIG. 6. Highly lithiated crystal showing extensive crystalline regions of the "124" phase, surrounded by an amorphous skin.

tween the "123" and "124" phases for higher lithium to "123" ratios, $0.50 \leq$ Li/"123" ≤ 1.2. For Li/"123" = 1.2, the "124" phase becomes predominant. As the "123", "124", and "247" phases essentially differ in the number of CuO chain layers along the *c*-axis (one in the case of the "123", two in the "124", and alternating one and two in the "247"), the transformation of the "123" structure into the "124" implies copper and oxygen diffusion in the structure or, alternatively, the outdiffusion of the other ions, or both. It is worth recalling here that a simple synthesis method for the "124" compound is the reaction of "123" with a stoichiometric amount of CuO at high temperature (810–830°C) (*11*). However, in the case of these "123" samples treated with *n*-BuLi, this transformation takes place *at room temperature* and without having added an excess of CuO to the initial "123" material. We may here remember that alkali–metal compounds are known to be good catalysts—even if, as yet, for unknown reasons—in the synthesis of "124" (*12*), but again high temperatures are required, which is not our case.

A possible reaction path for these lithium-induced room temperature transformations could involve a partial decomposition of the "123" phase, followed by a subsequent reorganization into the "124" structure. Although we do not know the intimate mechanism for such a process, it is certainly relevant in this context that Y_2BaCuO_5 appears as a by-product in the most lithiated samples, as observed both by its more intense X-ray diffraction peaks (*7*), and especially, by EDS analysis (unpublished results).

EELS analyses of the highly lithiated samples show that, as already suggested (*7*), lithium is present in the most reacted samples, i.e., those corresponding to the distorted "124" structure. This seems to show the implication of this chemical species in the reconstruction of "123" to "124" in the reaction of $YBa_2Cu_3O_{7-y}$ with *n*-BuLi. Work is in progress to establish the detailed process by which this reconstruction takes place.

The fact that lithium can be extracted so easily from the samples, together with the ionic conductivity displayed by these materials (*6*), suggests that lithium can readily move within the obtained materials. Size considerations allow us to explain this high mobility of lithium, in view of the large "124"-type tunnels that appear between two consecutive BaO layers formed in the portions of the structure where the extra CuO layer is located (Fig. 2, black arrows, and Fig. 9A).

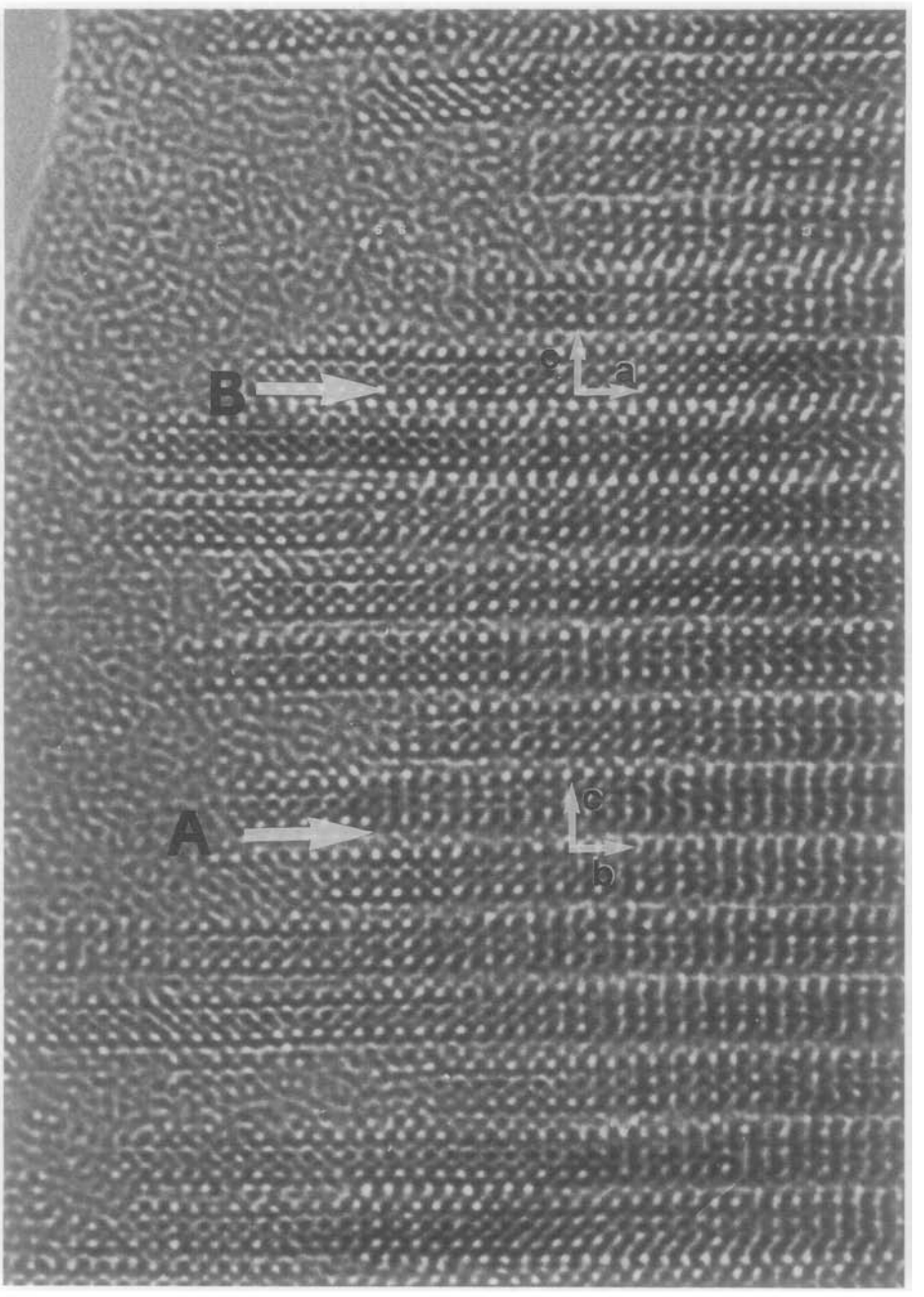

FIG. 7. Enlargement of zone I of Fig. 6, where the twinned nature of the obtained "124" phase can be clearly seen. Region A, zone axis [100]; region B, zone axis [010].

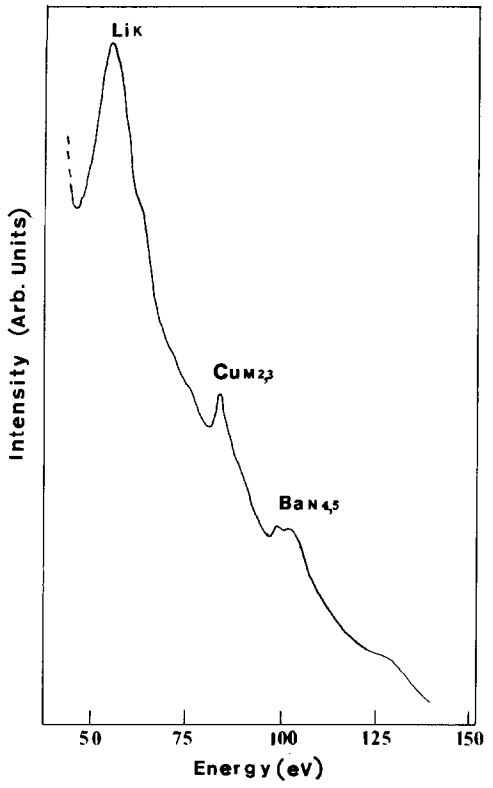

FIG. 8. Electron energy loss spectrum of the sample with a lithium to "123" molar ratio ≃ 1.2., at the energy range 40–150 eV. The Li *K*-edge is seen at ≃55 eV, the Cu $M_{2,3}$-edge at ≃85 eV, the Ba $N_{4,5}$-edge at ≃100 eV.

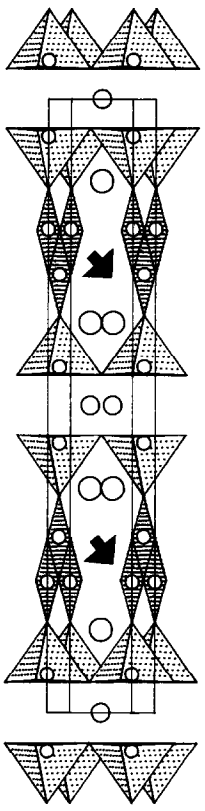

FIG. 9A. The structure of the $YBa_2Cu_4O_8$. The black arrows show the tunnels that exist between consecutive BaO planes.

Considering the "124" structure (*10*), we can see that these tunnels, extending between two consecutive BaO layers, are located along a line parallel to the *b*-axis and passing through the points $(\frac{1}{2}, b, \frac{1}{4})$. On the basis of the ionic, rigid sphere model, and taking into account the Shannon and Prewitt radii (*13*), we can see that these interstices have a minimum diameter of ≃1.0 Å along *a* between oxygen ions and ≃3.38 Å along *c* between the barium ions, while it is infinite in the *b* direction, Fig. 9B. This is to be compared with the diameters of 1.18, 1.52, and 1.84 Å for Li^+ in coordination numbers 4, 6, and 8, respectively. The fact that lithium is slightly bigger than the minimum

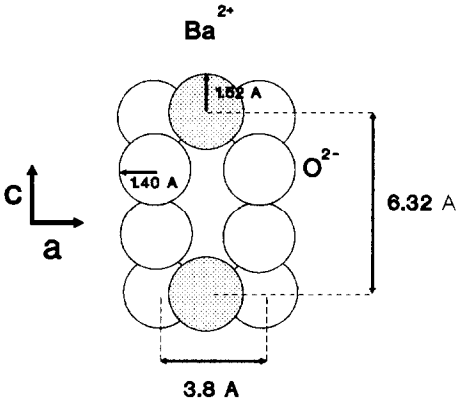

FIG. 9B. Cross section of the tunnel, viewing along the [010] direction, using the Shannon and Prewitt radii.

opening will certainly contribute to the observed activation energy obtained from AC conductivity measurements (*6*).

The EELS results, confirming the presence of lithium in the crystals, also support this idea of lithium diffusion taking place within the reconstructed "124"-type tunnels within the original "123" sample.

Acknowledgments

Financial support from CICYT (Project MAT 89/0768) and a grant to one of us (A.V.) from the MIDAS program are gratefully acknowledged. We also thank "Fundación Domingo Martínez" for a Research Award. We acknowledge the Centre for Electron Microscopy of our University for technical support.

References

1. C. Rosique-Pérez, J. González-Calbet, M. Vallet-Regí, and M. A. Alario-Franco, *J. Solid State Chem.* **76,** 313 (1988).
2. J. González-Calbet, C. Rosique-Pérez, M. Vallet-Regí, M. A. Alario-Franco, and J. Rodríguez-Carvajal, *Solid State Ionics* **32/33,** 162 (1989).
3. F. García-Alvarado, E. Morán, M. Vallet-Regí, J. González-Calbet, M. A. Alario-Franco, M. T. Pérez-Frías, J. L. Vicent, S. Ferrer, E. García-Michel, and M. C. Asensio, *Solid State Commun.* **63,** 507 (1987).
4. M. A. Alario-Franco, E. Morán, R. Saez-Puche, F. García-Alvarado, U. Amador, M. Barahona, F. Fernández, M. T. Pérez-Frías, and J. L. Vicent, *Mater. Res. Bull.* **23,** 313 (1988).
5. M. A. Alario-Franco, and C. Chaillout, *Solid State Ionics* **32/33,** 1056 (1989).
6. A. Várez, E. Morán, M. A. Alario-Franco, J. Santamaría, G. González-Díaz, and F. Sánchez-Quesada, *Solid State Commun.* **76,** 917 (1990).
7. M. A. Alario-Franco, E. Morán, A. Várez, J. Santamaría, and F. Sánchez-Quesada, *Solid State Ionics* **44,** 73 (1990).
8. J. Vondrák, I. Jakubec, J. Bludská, and V. Skácel, *Electrochim. Acta* **35,** 995 (1990).
9. M. Vallet-Regí, J. González-Calbet, M. A. Alario-Franco, J. C. Grenier, and P. Hagenmuller, *J. Solid State Chem.* **55,** 251 (1984).
10. P. Bordet, J. L. Hodeau, R. Argoud, J. Muller, M. Marezio, J. C. Martínez, J. J. Prejean, J. Karpinski, E. Kaldis, S. Rusiecki, and B. Bucher, *Physica C* **162–4,** 524 (1989).
11. S. Jin, H. M. O'Bryan, P. K. Gallagher, T. H. Tiefel, R. J. Cava, R. A. Fastnacht, and G. W. Kammlott, *Physica C* **165,** 415 (1990).
12. D. M. Pooke, R. G. Buckley, M. R. Presland, and J. L. Tallon, *Phys. Rev. B* **41,** 6616 (1990).
13. R. D. Shannon and C. T. Prewitt, *Acta Crystallogr., Sect. B: Struct. Sci.* **B25,** 925 (1969).